



Interconversion between guanine quartets and triads on the Au(111) surface†

Cite this: DOI: 10.1039/d2cc00060a

Yuanqi Ding,^a Lei Xie,^a Donglin Li,^a Hanlin Shen,^a Cuiyu Li^b and Wei Xu^{id}*^a

Received 5th January 2022,
Accepted 10th February 2022

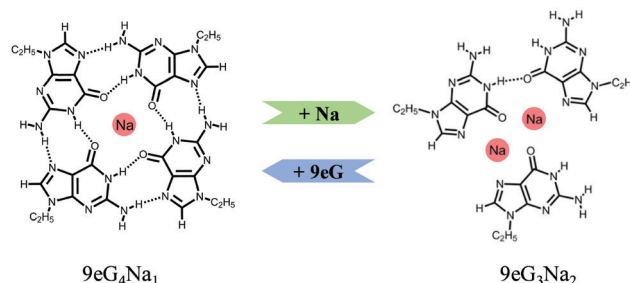
DOI: 10.1039/d2cc00060a

rsc.li/chemcomm

Based on STM imaging and DFT calculations, we show the real-space experimental evidence of the interconversion between G-quartets and G-triads on the Au(111) surface, and further reveal the relative stabilities of these two elementary motifs, which helps to increase the fundamental understanding of the relationship between G-triplex and G-quadruplex DNA structures.

The structural polymorphism of DNA molecules (*e.g.* duplexes,¹ triplexes,² quadruplexes,³ hairpins,⁴ cruciform,⁵ and i-motif,⁶ *etc.*) plays a pivotal role in regulating cellular functions and biological processes. The conformations and relationships of various DNA forms have attracted tremendous interest over the past few decades.^{7–9} Among others, the well-known guanine(G)-quadruplexes stacked by G-quartets stabilized by cations are involved in areas ranging from structural biology to medicinal chemistry, and thus have been extensively studied.³ In some spectroscopic research studies^{10–12} and theoretical predictions,^{13,14} the G-triplex is considered to be a kind of folding intermediate of the G-quadruplex, which is formed by G-triad planes also stabilized by cations in solution.^{8,15} The corresponding building blocks of G-triplex and G-quadruplex structures, *i.e.*, G-triad and G-quartet, respectively, have also been introduced to the surface science community and investigated by scanning tunneling microscopy (STM).^{16–22} However, to the best of our knowledge, the relationship of these two structures has not been determined experimentally. Thus, it is of general interest to construct a system under well-controlled ultrahigh vacuum (UHV) conditions with the aim of building up these two elementary structural motifs and exploring the possible interconversion between G-triads and G-quartets; such real-space evidence may provide insights into biologically relevant issues.

In this study, we choose the derivative of the DNA base, 9-ethylguanine molecules (shortened as 9eG, modified at the same derived site as that of the natural nucleosides) and alkali metal sodium (Na) as a model system. The Au(111) surface is employed as a template to ensure the flat adsorption geometries of the molecules and facilitate the formation of planar triad and quartet structures, on which the potential interconversion between these two elementary structural motifs could be explored. Herein, from the interplay of high-resolution STM imaging and density functional theory (DFT) calculations, we show the formation of the 9eG₄Na₁ quartet and 9eG₃Na₂ triad stabilized by a combination of hydrogen bonds and ionic bonds, and moreover, the interconversion between these two motifs in response to the ratio of 9eG/Na is achieved (*cf.* Scheme 1). DFT calculations further validate that the 9eG₄Na₁ quartet (with the binding energy of 1.45 eV per molecule) is energetically more favorable than the 9eG₃Na₂ triad (with the binding energy of 1.33 eV per molecule), which is consistent with the experimental observations that the 9eG₄Na₁ quartet is thermodynamically more stable than the 9eG₃Na₂ triad when sufficient 9eG molecules are provided. This study demonstrates the real-space experimental evidence on the interconversion between a G-triad and G-quartet, which may shed light on the understanding of the relationship between G-triplex and G-quadruplex DNA structures.



Scheme 1 Schematic illustration of the interconversion between a 9eG₄Na₁ quartet and 9eG₃Na₂ triad on the Au(111) surface.

^a Interdisciplinary Materials Research Center, College of Materials Science and Engineering, Tongji University, Shanghai 201804, P. R. China.
E-mail: xuwei@tongji.edu.cn

^b Advanced Computing East China Sub-Center, Suma Technology Co., Ltd., Kunshan 215300, P. R. China

† Electronic supplementary information (ESI) available. See DOI: 10.1039/d2cc00060a

Firstly, stepwise deposition of metal Na on the 9eG islands has been performed, and the structural transformation from the $9eG_4Na_1$ network to the $9eG_3Na_2$ one is achieved on the Au(111) surface, as shown in Fig. 1a–d. Reversibly, the $9eG_3Na_2$ network could be transformed back to the $9eG_4Na_1$ one by adding more 9eG molecules (Fig. 1d–f). With such a sequential deposition method, the interconversion between G-triad and G-quartet motifs is achieved on the Au(111) surface. The corresponding STM images and DFT calculated models will be discussed in detail in the following.

Deposition of metal Na on the 9eG-precovered Au(111) surface followed by annealing at 350 K leads to the formation of a grid-like network structure, as shown in Fig. 2a. The close-up STM image (Fig. 2b) shows that such a network is composed of pure $9eG_4Na_1$ quartet structural motifs with four 9eG molecules in homochirality, and a similar structure (prepared by 9eG molecules and NaCl salt) has been previously reported by our group.²¹ From the DFT-optimized model superimposed on the STM images (Fig. 2c and d), it can be identified that the $9eG_4Na_1$ quartet is stabilized by a combination of hydrogen bonds and ionic bonds, and the quartets are further linked with each other *via* van der Waals interactions from the ethyl groups of the 9eG molecules.

Subsequent deposition of additional Na on the $9eG_4Na_1$ -precovered surface followed by annealing at 350 K leads to the structural transformation from the grid-like network to another porous one (Fig. 3a). The close-up STM image (Fig. 3b) provides more details of the structure, which reveals that the porous network is composed of triads (depicted by blue contours in Fig. 3b), and the chirality of the three molecules in the triad can be distinguished as indicated by R and L notations; thus the triad is a heterochiral motif. Note that two Na cations in the triads can be clearly identified in a special tip state under the scanning condition of the negative bias, as illustrated in Fig. S1 (ESI†). Based on the above analysis, DFT calculations are

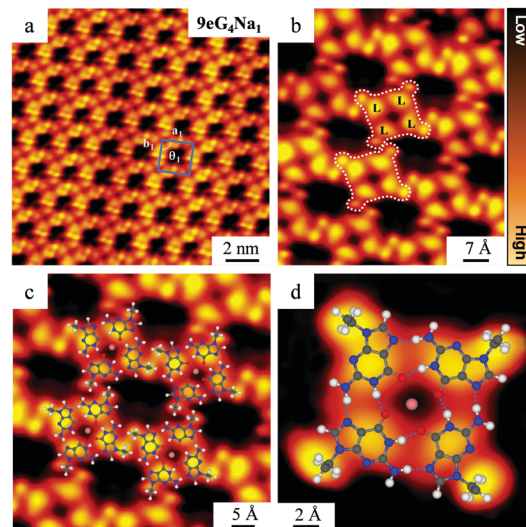


Fig. 2 STM images and DFT-optimized structural models showing the formation of $9eG_4Na_1$ quartets on Au(111). (a) A large-scale STM image showing the grid-like structure composed of $9eG_4Na_1$ quartets. The indicated unit cell has parameters $a_1 = 18.5 \pm 0.1 \text{ \AA}$, $b_1 = 18.5 \pm 0.1 \text{ \AA}$, $\theta_1 = 90^\circ \pm 1^\circ$. (b) A close-up STM image allowing the individual $9eG_4Na_1$ quartet (depicted by white contours) and the homochirality of 9eG molecules within the quartet (indicated by L notations) to be distinguished. (c) The STM image with the superimposed DFT-optimized model showing interconnections of quartets (i.e., van der Waals interactions from ethyl groups). (d) A close-up STM image of the $9eG_4Na_1$ quartet superimposed with the DFT-optimized model. Hydrogen bonds are depicted by blue dashed lines. H: white; C: gray; N: blue; O: red; Na: pink. Scanning conditions: $I_t = 0.70 \text{ nA}$, $V_t = 1400 \text{ mV}$.

performed to build up the atomic-scale models on the triad-network. From the high-resolution STM image and the superimposed structural model shown in Fig. 3d, the triad is attributed to a $9eG_3Na_2$ motif, in which the ionic bonds between Na cations and 9eG molecules together with the $NH \cdots O$ hydrogen bond contribute to the stabilization of the triad motif.

Moreover, from the DFT-optimized model of the $9eG_3Na_2$ network superimposed on the STM image (Fig. 3c), we identify that the triads are linked with the adjacent ones *via* the double $NH \cdots N$ hydrogen bonds between 9eG molecules (depicted by blue dashed lines in Fig. 3c).

Interestingly, controllable deposition of 9eG molecules on the $9eG_3Na_2$ -precovered surface followed by annealing at 350 K leads to the formation of a square block network structure, as shown in Fig. 4a. Closer inspection of the structure (Fig. 4b) shows that such a network is composed of both quartets and triads as depicted by white and blue contours, respectively. This means that deposition of additional 9eG molecules leads to the structural transformation from triads back to quartets. The defects shown in Fig. S2 (ESI†) could also help to ensure the two kinds of elementary motifs. Based on this analysis, the square block network is attributed to a hybrid supramolecular network composed of both $9eG_4Na_1$ and $9eG_3Na_2$ motifs, and the DFT calculations are performed to build up the atomic-scale model of the network. From the close-up STM image and the

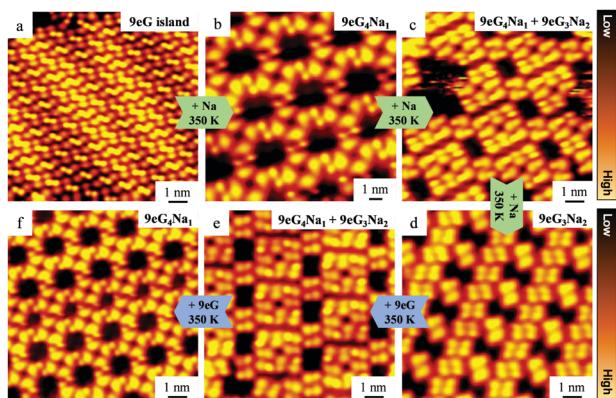


Fig. 1 STM images showing the reversible structural transformations in response to the ratio of metal Na and 9eG molecules. (a) Formation of the 9eG island on Au(111) at room temperature. (b–d) Structural transformations from the $9eG_4Na_1$ network over the mixture of $9eG_4Na_1$ and $9eG_3Na_2$ network to the $9eG_3Na_2$ network on the Au(111) surface. (d–f) The corresponding reversed structural transformation. Scanning conditions: $I_t = 0.80 \text{ nA}$, $V_t = 1400 \text{ mV}$.

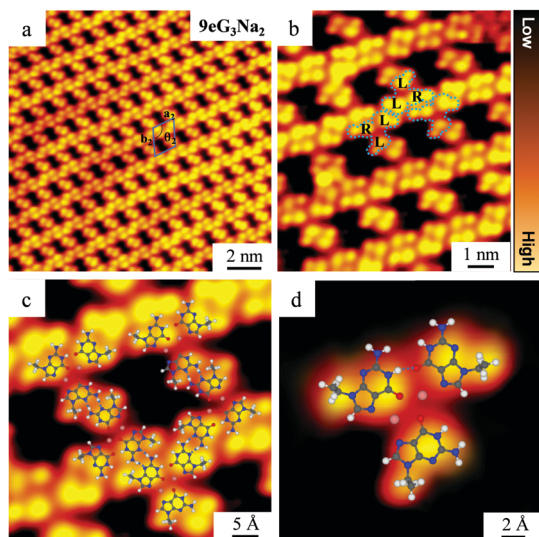


Fig. 3 STM images and DFT-optimized structural models showing the formation of $9eG_3Na_2$ triads on Au(111). (a) A large-scale STM image showing the porous network structure composed of $9eG_3Na_2$ triads. The indicated unit cell has parameters $a_2 = 20.5 \pm 0.1$ Å, $b_2 = 28.7 \pm 0.1$ Å, $\theta_2 = 114^\circ \pm 1^\circ$. (b) A close-up STM image allowing the individual triad (depicted by blue contours) and the chirality of each 9eG molecule within a triad (indicated by R and L notations) to be distinguished. (c) The STM image with the superimposed DFT-optimized model shows interconnections of the triads (double $NH \cdots N$ hydrogen bonds). (d) A close-up STM image of the $9eG_3Na_2$ triad superimposed with the DFT-optimized model. Hydrogen bonds are depicted by blue dashed lines. H: white; C: gray; N: blue; O: red; Na: pink. Scanning conditions: $I_t = 1.10$ nA, $V_t = 1400$ mV.

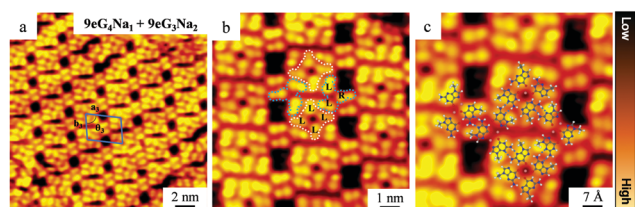


Fig. 4 STM images and DFT-optimized structural models showing the formation of a hybrid supramolecular network composed of $9eG_4Na_1$ quartets and $9eG_3Na_2$ triads on Au(111). (a) A large-scale STM image showing the square block network structure. The indicated unit cell has parameters $a_3 = 31.8 \pm 0.1$ Å, $b_3 = 24.7 \pm 0.1$ Å, $\theta_3 = 79^\circ \pm 1^\circ$. (b) A close-up STM image allowing the individual $9eG_4Na_1$ and $9eG_3Na_2$ motifs (depicted by white and blue contours, respectively) and the chirality of each 9eG molecule (indicated by R and L notations) to be distinguished. (c) A close-up STM image with the superimposed DFT-optimized model showing interconnections between quartets and triads (double $NH \cdots N$ hydrogen bonds depicted by blue dashed lines). H: white; C: gray; N: blue; O: red; Na: pink. Scanning conditions: $I_t = 0.80$ nA, $V_t = 1700$ mV.

superimposed structural model shown in Fig. 4c, we identify that the $9eG_4Na_1$ quartet and the $9eG_3Na_2$ triad are linked *via* double $NH \cdots N$ hydrogen bonds between 9eG molecules (depicted by blue dashed lines in Fig. 4c). Further deposition of more 9eG molecules leads to the complete structural transformation to the $9eG_4Na_1$ quartet network, as shown in Fig. 1e and f.

Based on the above experimental observations on the formation of various network structures shown in Fig. 1, we draw the conclusion that the well-controlled interconversion between $9eG_4Na_1$ quartets and $9eG_3Na_2$ triads is achieved by the regulation of the 9eG/Na ratio on the Au(111) surface. Note that the interconversion between quartet and triad also proves the reversibility of ionic bonds and hydrogen bonds. And more importantly, it suggests that the formation of the $9eG_4Na_1$ quartet is thermodynamically more favorable than that of the $9eG_3Na_2$ triad when sufficient 9eG molecules are provided on the surface.

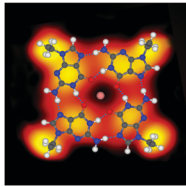
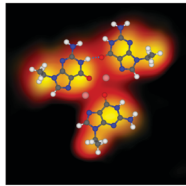
To further quantify the relationship of the quartet and triad motifs, we then perform calculations on the binding energy (E_b) of the $9eG_4Na_1$ and $9eG_3Na_2$ motifs in the gas phase to characterize their relative stabilities (Table 1). E_b is defined as the total energy of the whole relaxed system (E_{sys} , including the hydrogen bonds and ionic bonds in this system) minus the total energies of all of the individual relaxed components (E_{com}), that is, $E_b = E_{sys} - E_{com}$. The E_b value of the $9eG_4Na_1$ motif is calculated to be 1.45 eV per molecule, and the E_b value of the $9eG_3Na_2$ motif is calculated to be 1.33 eV per molecule, which is in accordance with the experimental results. More details of the calculations can be found in Table S1 (ESI†).

In conclusion, by the combination of STM imaging and DFT calculations, we present the real-space experimental evidence of the interconversion between a G-triad and G-quartet on the Au(111) surface with the trigger of the G/Na ratio, and further reveal the relative stabilities of these two elementary motifs. Such real-space evidence may help to increase our fundamental understanding of the G-triplex and G-quadruplex DNA structures.

W. X. conceived and designed the experiments. Y. D., L. X., D. L. and H. S. performed the STM experiments. Y. D. and C. L. did the DFT calculations. W. X. and Y. D. analyzed the data. W. X. and Y. D. drafted the manuscript. All authors proofread, commented on, and approved the final version of the manuscript.

The authors acknowledge financial support from the National Natural Science Foundation of China (Grants No. 22125203, 21790351, 22102117, 22002183).

Table 1 Binding energy (E_b) of the $9eG_4Na_1$ and $9eG_3Na_2$ motifs in the gas phase with the corresponding STM images and structural models

Binding energy (E_b)	
$9eG_4Na_1$	$9eG_3Na_2$
	
1.45 eV/molecule	1.33 eV/molecule

Conflicts of interest

The authors declare that they have no conflict of interest in this work.

Notes and references

- 1 J. D. Watson and F. H. C. Crick, *Nature*, 1953, **171**, 737.
- 2 V. Sklenar and J. Feigon, *Nature*, 1990, **345**, 836.
- 3 J. T. Davis, *Angew. Chem., Int. Ed.*, 2004, **43**, 668.
- 4 D. Christophe, *Nature*, 1988, **333**, 214.
- 5 N. Panayotatos and R. D. Wells, *Nature*, 1981, **289**, 466.
- 6 M. Guéron and J.-L. Leroy, *Curr. Opin. Struct. Biol.*, 2000, **10**, 326.
- 7 A. Rajendran, M. Endo, K. Hidaka and H. Sugiyama, *Angew. Chem., Int. Ed.*, 2014, **53**, 4107.
- 8 H. X. Jiang, Y. Cui, T. Zhao, H. W. Fu, D. Koirala, J. A. Punnoose, D. M. Kong and H. Mao, *Sci. Rep.*, 2015, **5**, 9255.
- 9 A. Rajendran, M. Endo, K. Hidaka, M. P. Teulade-Fichou, J. L. Mergny and H. Sugiyama, *Chem. Commun.*, 2015, **51**, 9181.
- 10 Z. Zhang, J. Dai, E. Veliath, R. A. Jones and D. Yang, *Nucleic Acids Res.*, 2010, **38**, 1009.
- 11 D. Koirala, T. Mashimo, Y. Sannohe, Z. Yu, H. Mao and H. Sugiyama, *Chem. Commun.*, 2012, **48**, 2006.
- 12 R. D. Gray, J. O. Trent and J. B. Chaires, *J. Mol. Biol.*, 2014, **426**, 1629.
- 13 T. Mashimo, H. Yagi, Y. Sannohe, A. Rajendran and H. Sugiyama, *J. Am. Chem. Soc.*, 2010, **132**, 14910.
- 14 V. Limongelli, S. De Tito, L. Cerofolini, M. Fragai, B. Pagano, R. Trotta, S. Cosconati, L. Marinelli, E. Novellino, I. Bertini, A. Randazzo, C. Luchinat and M. Parrinello, *Angew. Chem., Int. Ed.*, 2013, **52**, 2269.
- 15 L. Cerofolini, J. Amato, A. Giachetti, V. Limongelli, E. Novellino, M. Parrinello, M. Fragai, A. Randazzo and C. Luchinat, *Nucleic Acids Res.*, 2014, **42**, 13393.
- 16 W. Xu, R. E. A. Kelly, H. Gersen, E. Lægsgaard, I. Stensgaard, L. N. Kantorovich and F. Besenbacher, *Small*, 2009, **5**, 1952.
- 17 A. Ciesielski, S. Lena, S. Masiero, G. P. Spada and P. Samori, *Angew. Chem., Int. Ed.*, 2010, **49**, 1963.
- 18 D. González-Rodríguez, P. G. A. Janssen, R. Martín-Rapún, I. De Cat, S. De Feyter, A. P. Schenning and E. W. Meijer, *J. Am. Chem. Soc.*, 2010, **132**, 4710.
- 19 W. Xu, J. G. Wang, M. Yu, E. Lægsgaard, I. Stensgaard, T. R. Linderth, B. Hammer, C. Wang and F. Besenbacher, *J. Am. Chem. Soc.*, 2010, **132**, 15927.
- 20 W. Xu, Q. Tan, M. Yu, Q. Sun, H. Kong, E. Lægsgaard, I. Stensgaard, J. Kjems, J.-G. Wang, C. Wang and F. Besenbacher, *Chem. Commun.*, 2013, **49**, 7210.
- 21 C. Zhang, L. Wang, L. Xie, H. Kong, Q. Tan, L. Cai, Q. Sun and W. Xu, *Chem. Phys. Chem.*, 2015, **16**, 2099.
- 22 N. Bilbao, I. Destoop, S. De Feyter and D. Gonzalez-Rodriguez, *Angew. Chem., Int. Ed.*, 2016, **55**, 659.